Science of the Total Environment 701 (2020) 134877

Contents lists available at ScienceDirect

Science of the Total Environment

journal homepage: www.elsevier.com/locate/scitotenv

Modeling forest management effects on water and sediment yield from nested, paired watersheds in the interior Pacific Northwest, USA using WEPP

A. Srivastava [a,*], E.S. Brooks [b], M. Dobre [b], W.J. Elliot [c], J.Q. Wu [d], D.C. Flanagan [e], J.A. Gravelle [f], T.E. Link [g]

[a] Department of Agricultural and Biological Engineering, Purdue University, West Lafayette, IN, USA
[b] Department of Soil and Water Systems, University of Idaho, Moscow, ID, USA
[c] USDA-Forest Service, Rocky Mountain Research Station, Moscow, ID, USA
[d] Department of Biological Systems Engineering, Puyallup Research and Extension Center, Washington State University, Puyallup, WA, USA
[e] USDA-Agricultural Research Service, National Soil Erosion Research Laboratory, West Lafayette, IN, USA
[f] Environmental Resource Consultant, Pine Orchard Inc., Moscow, ID, USA
[g] College of Natural Resources, University of Idaho, Moscow, ID, USA

HIGHLIGHTS

- WEPP modeling was conducted on paired, nested watersheds with forest managements.
- WEPP-simulated daily streamflow was in close agreement with observed values.
- WEPP captured water and sediment yields and changes due to harvesting practices.
- Results demonstrated WEPP's potential as a decision-aid tool in forest management.

GRAPHICAL ABSTRACT

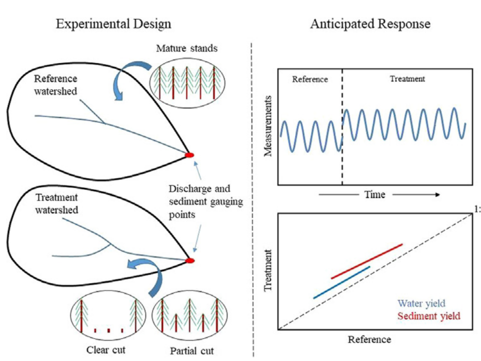

ARTICLE INFO

Article history:
Received 12 August 2019
Received in revised form 4 October 2019
Accepted 6 October 2019
Available online 1 November 2019

Editor: Ashantha Goonetilleke

Keywords:
Forest harvesting
Hydrology
Sediment transport
Physically-based model
WEPP

ABSTRACT

The Water Erosion Prediction Project (WEPP) model was applied to seven paired, nested watersheds within the Mica Creek Experimental Watershed located in northern Idaho, USA. The goal was to evaluate the ability of WEPP to simulate the direct and cumulative effects of clear-cutting and partial-cutting (50% canopy removal) on water and sediment yield. WEPP was modified to better represent changes in the Leaf Area Index during post-harvest forest vegetative recovery. Good agreement between simulated and observed streamflow was achieved with minimal to no calibration over a 16-year (1992–2007) period. For the seven watersheds and the entire study period, the overall Nash-Sutcliffe Efficiency (*NSE*), Kling-Gupta efficiency (*KGE*), and deviation of runoff volume (D_V) between observed and simulated daily streamflow ranged 0.58–0.71, 0.67–0.81, and −4% to 9%, respectively. Good agreement between predicted and observed suspended sediment yield was achieved through the calibration of a single channel critical shear stress parameter. For sediment yield, *NSE*, *KGE*, and D_V ranged 0.62–0.97, 0.43–0.97, and −2% to 2%, respectively, for the calibration period, and 0.61–0.93, 0.42–0.95, and −24% to 13%, respectively, for the period of model performance assessment. Regression analysis of observed- and WEPP-simulated increase in water and sediment yield following clear-cut treatment was similar; however, the WEPP-simulated increase was lower compared to observations particularly from the partial-cut

* Corresponding author at: 275 South Russell Street, Purdue University, West Lafayette, IN 47907, USA.
E-mail addresses: srivas42@purdue.edu (A. Srivastava), ebrooks@uidaho.edu (E.S. Brooks), mdobre@uidaho.edu (M. Dobre), welliot@moscow.com (W.J. Elliot), jwu@wsu.edu (J.Q. Wu), dennis.flanagan@ars.usda.gov (D.C. Flanagan), jag@pineorchard.com (J.A. Gravelle), tlink@uidaho.edu (T.E. Link).

https://doi.org/10.1016/j.scitotenv.2019.134877

watershed. The variability in the critical shear parameter for different stream channels in the study watersheds was directly related to the observed mean particle size on the stream bed and suggests that applications of the WEPP model in ungauged basins could potentially set the critical shear parameter based on particle size. Overall, the simulated results demonstrate the potential of WEPP as a modeling tool for forestland watershed management, particularly for estimating the effects of forest harvest on hydrograph fluctuations and consequently, stream sediment transport.

1. Introduction

Forest operations including harvesting and road constructions can significantly impact hydrology and sediment transport at the hillslope and watershed scale (Moore and Wondzell, 2005; Gomi et al., 2005; Hassan et al., 2005; Hancock et al., 2017; Hatten et al., 2018). Forest harvest influences soil water retention and permeability, pore pressure modification, hillslope soil saturated hydraulic conductivity (Ziegler et al., 2006; Terwilliger, 1990; Shao et al., 2018; Ni et al., 2019), and root decay causing causing an increase in soil instability (O'Loughlin, 1974; Bischetti et al., 2016; Cislaghi et al., 2019). Consequently, forest management activities can greatly affect peak streamflow (Jones and Grant, 1996; Jones and Post, 2004; Moore and Wondzell, 2005; Troendle et al., 2010; Schnorbus and Alila, 2013), and annual water and sediment yield (Moore and Wondzell, 2005; Gomi et al., 2005; Swank et al., 2014; Bathurst and Iroume, 2014; Bywater-Reyes et al., 2018) through changes in dominant hydrological processes and flow paths. It is generally recognized that forest harvesting reduces interception loss and plant transpiration leading to increased soil moisture, peak streamflow, and water yield (Bosch and Hewlett, 1982; Troendle et al., 2001; Jones and Post, 2004; Moore and Wondzell, 2005; Boggs et al., 2015; Stednick and Troendle, 2016). Increased soil loss from forest operations may be due to exposure of erodible mineral soil at the soil surface (Elliot, 2013; Troendle et al., 2010). Unless severe disturbances occur from harvesting, the majority of upland erosion during logging activities is generated in road construction and skid trail areas where soils are highly compacted causing decreased soil hydraulic conductivity and increased infiltration-excess overland flow (Gomi et al., 2005). Increased peak streamflow after logging can also lead to increased stream sediment transport from the stream bed and banks (Gomi et al., 2005, Bathurst and Iroume, 2014; Hancock et al., 2017; Bywater-Reyes et al., 2018).

There is an increased demand for quantifying the impacts of forest management practices on water and sediment yield to ensure long-term sustainability of forest resources in the mountainous watersheds of the Pacific Northwest of the USA (Waichler et al., 2005; Abdelnour et al., 2011; Du et al., 2013; Elliot, 2013; Brooks et al., 2016; Hancock et al., 2017). The impacts of management practices on watershed hydrological response and sediment transport depends on harvesting locations and amount, and climate regimes in a watershed (Stednick, 1996; Stednick and Troendle, 2016). Due to the spatiotemporal variability of hydrological patterns and processes that control streamflow and sediment transport, and the high costs associated with monitoring these processes, numerical models are widely used as cost-effective tools for assessing the potential impacts of management practices on watershed processes (Aksoy and Kavvas, 2005; Beckers et al., 2009; Anderson and Lockaby, 2011; Bourdin et al., 2012; Golden et al., 2016; Tegegne et al., 2017). For example, Abdelnour et al. (2011) assessed the impact of harvest location in a watershed on hydrological responses using the Visualizing Ecosystems for Land Management Assessments (VELMA) model. Du et al. (2016) used the Distributed Hydrology-Soil-Vegetation Model (DHSVM) to evaluate the hydrologic effects of forest harvest and recovery. Istanbulluoglu et al. (2004) applied the numerical model to estimate the effects of spatial distribution of forest vegetation and disturbances on sediment yield.

The Water Erosion Prediction Project (WEPP) model is a physically-based hydrology and erosion prediction technology developed by the US Department of Agriculture (Flanagan and Nearing, 1995, Flanagan et al., 2007), which has been developed as a decision-support tool at the hillslope scale for forest and wildfire activities (Robichaud et al., 2007; Elliot, 2004; Elliot et al., 2007) (https://forest.moscowfsl.wsu.edu/fswepp/). The model is built on the fundamentals of hydrology, plant science, hydraulics, and erosion mechanics (Flanagan and Nearing, 1995). Applications of the WEPP model to watersheds were initially limited to small catchments (<5 km^2) (Covert et al., 2005; Conroy et al., 2006; Dun et al., 2009) due to the simplistic peak streamflow algorithms and the lack of ability to represent baseflow in the model. By incorporating a simple linear reservoir algorithm to represent the interaction between groundwater storage and baseflow and taking the cumulative output from all hillslopes rather than using stream routing algorithms to assess attenuation in hillslope runoff output to the watershed outlet, Srivastava et al. (2013, 2017, and 2018) and Brooks et al. (2016) showed good agreement between simulated and observed streamflow from watersheds varying in size from 5 km^2 to 36 km^2. The recent development and implementation of more appropriate channel routing methods (kinematic-wave and the Muskingum-Cunge) for perennial streams (Wang et al., 2014) allows WEPP to generate peak flows at sub-daily time steps and provides an opportunity to assess the ability of the model to predict stream sediment transport from large watersheds.

To date, all the aforementioned WEPP watershed applications have been focused on simulating streamflow from undisturbed watersheds. However, the recent model improvements provided a great opportunity to evaluate WEPP's ability to simulate the effects of forest management changes on watershed hydrology and sediment transport. In the last several decades, a comprehensive investigation of direct and cumulative effects of forest management activities on hydrology and sediment transport has been carried out by the Potlatch Corporation in the Mica Creek Experimental Watershed (47°09′N, 116°16′W) located in Shoshone County, northern Idaho, USA (Gravelle and Link, 2007) (Fig. 1). To evaluate the effectiveness of Idaho Forest Practice Act regulations and contemporary Best Management Practices (BMPs) (Barkley et al., 2015), both road construction associated with timber harvest and different harvesting methods (clear-cut and partial-cut) were studied. A sampling design with before-after-control-impact/treat ment (BACI) approach (Eberhardt, 1976) in nested and paired watersheds was used to collect streamflow and sediment at seven watershed outlets before the road construction and timber harvesting, after road construction, and after harvesting (Chen et al., 2005; Hubbart et al., 2007a). In this study, we applied the WEPP model to the Mica Creek Experimental Watershed and evaluated its ability to simulate the effects of forest management practices on water and sediment yield. Specifically, we evaluated model's

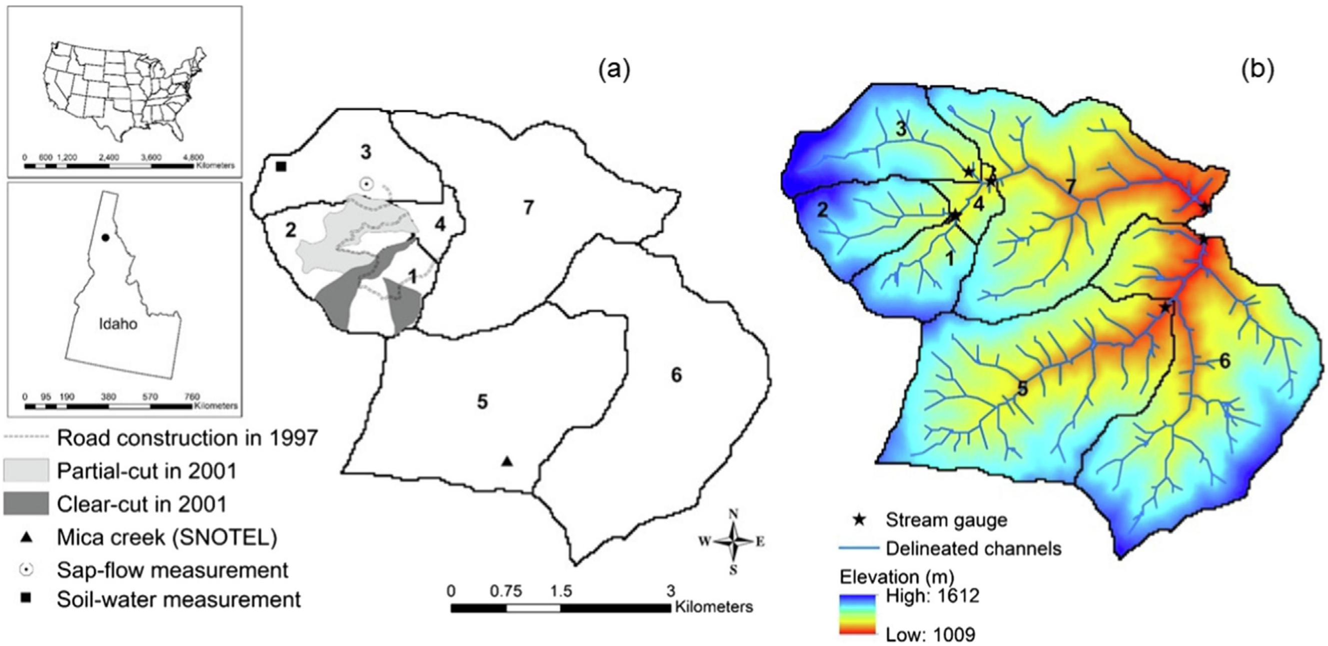

Fig. 1. Mica Creek Experimental Forest (MCEW) watershed, Idaho, USA: (a) clear-cut and partial-cut harvesting areas, roads construction, and field-measurement points and (b) topography, stream gauges, and WEPP-delineated channels. Watersheds (WS) 1 with clear-cut and WS 2 with partial-cut are paired with undisturbed reference WS 3. WS 4 and 7 are paired with WS 5 and 6, respectively.

performance for undisturbed reference watershed conditions, and simulated water and sediment yield for pre- and post-harvest treatment conditions. To the Authors' knowledge, this is the first comprehensive assessment of the algorithms for stream channel routing and sediment transport in WEPP for a large forested watershed. Since the WEPP model can be successfully applied in ungauged watersheds (Brooks et al., 2016), this study will help land managers better understand the effects of forest management changes to both streamflow and sediment yield.

2. Methods

2.1. Watershed description

The Mica Creek Experimental Watershed (MCEW) is 25 km^2 in size, with elevations ranging 1000–1600 m a.m.s.l., and is situated in a transitional climate zone impacted by both continental and maritime hydrometeorological conditions. Based on nearby USDA NRCS SNOw TELemetry (SNOTEL) data located at 1375 m a.m.s.l. in watershed 5 (Fig. 1), the average annual precipitation is 1450 mm with approximately 70% falling as snow (USDA NRCS, 2016). The annual average temperature is 4.9 °C, with a monthly average maximum of 24.6 °C in August and a monthly average minimum of −5.6 °C in December. The study area is in complex mountainous terrain with V-shaped valleys and generally 15–40% moderately sloped hillsides. The existing Bouldercreek silt loam (*ashy over loamy-skeletal, amorphic over isotic, frigid typic udivitrands*) soil series is deep and well drained and varies from gravelly to extremely gravelly over the soil profile depth of 1524 mm (USDA NRCS, 2014). These soils were formed in colluvium and residuum weathered from schist, gneiss, granitic or quartzite bedrock, with a thick mantle of volcanic ash and loess (USDA NRCS, 2014). The current vegetation was comprised mostly of 65- to 75-year-old mixed-species conifer stands, including Douglas-fir (*Pseudotsuga menziesii*), western hemlock (*Tsuga heterophylla*), western larch (*Larix occidentalis*), western red cedar (*Thuja plicata*), grand fir (*Abies grandis*), western white pine (*Pinus monticola*), and Engelmann spruce (*Picea engelmannii*). These overstory coniferous trees have an average canopy height of 35 m, canopy cover of 90% and Leaf Area Index (*LAI*) of 7 m^2 m^{-2} (Hubbart et al., 2007b). Grasses, forbs, and shrubs form most of the understory vegetation (Hubbart et al., 2007b).

The Mica Creek project was designed by the Potlatch Corporation as a paired and nested watershed study to evaluate the direct and cumulative effects of timber harvest and road construction (Fig. 1). Watershed (WS) 3, an undisturbed reference watershed, was paired with WS 1 and WS 2. WS 4 (encompassing WS 1, 2, and 3) was paired with undisturbed reference WS 5, and WS 7 (including WS 1, 2, 3, and 4) was paired with undisturbed reference WS 6. WS 3 was intended to retain background conditions against which forest harvesting activities in WS 1 and WS 2 were evaluated concerning their direct effects on hydrology and water quality (Hubbart et al., 2007a). WS 5 and WS 6 were intended to evaluate the cumulative hydrologic and erosion effects of the treatments in WS 1 and WS 2. These paired watersheds were located as adjacent catchments with similar vegetation within the headwaters of West Fork Mica Creek, as they were all subject to the same harvest practices during the 1920s and 1930s. Since that time, the watersheds remained undisturbed and vegetation were allowed to re-establish to second growth forest of mixed conifers and other herbaceous vegetation within riparian zones without human disturbances for nearly seven decades (Hubbart et al., 2007b). Other characteristics including topography (Table B1), soil, and geology in paired watersheds were comparable.

WS 1 and 2 underwent road construction in September 1997 for timber harvesting (Karwan et al., 2007). The fraction of road was 2 to 3% of the watershed area in WS 1 and 2. In WS 1, 50% of the drainage area was clear-cut between July and October 2001, and then broadcast-burned and replanted in May 2003. WS 2 experienced an overall 25% vegetative (canopy cover) removal from a partial-cut harvesting over 50% of the drainage area in the fall of 2001. Timber harvesting activities were conducted in accordance with Idaho Forest Practice Act guidelines retaining 22.86 m of streamside management zones on each side of streams to prevent sediment reaching water bodies.

2.2. Data collection and processing

Streamflow and total suspended solids (TSS) were recorded at the seven flume locations (Fig. 1). Streamflow was measured using Parshall flumes with a nitrogen bubbler-type pressure transducer system (Riverside Technology Inc., Fort Collins, Colorado) at a 30-min interval, and recorded with a Campbell Scientific CR10 datalogger (Campbell Scientific Inc., Logan, Utah) (Hubbart et al., 2007a). Water samples were collected using ISCO 3700 automatic samplers at variable time intervals. Samples were taken two to three times each day during high-flow periods of spring snowmelt and on a biweekly basis during low-flow periods in summer and early fall. Collected samples were analyzed for TSS following the American Water Works Association (1989) guidelines. A detailed description of data collection and analysis can be found in Karwan et al. (2007). Upstream of each flume, Wolman pebble counts were made once a year in the summer or fall from 1992 to 2005 to evaluate the particle-size distribution of channel materials. Bedload was not measured in this study.

Observed 30-min discharge data during October 1991 through September 2007 were aggregated to daily values for WEPP model assessment. To compare WEPP-simulated sediment yields with observations, instantaneous observed TSS values were converted to daily sediment loadings using the LOAD ESTimator (LOADEST; Runkel et al., 2004). For our study, an automated model selection option was chosen in LOADEST to select the best model from the set of available nine predefined regression models. LOADEST uses regression to derive a relationship between discharge and water quality data. This relationship was further used to estimate loadings on days where water quality data are unavailable. Continuous sediment loads were estimated using the adjusted maximum likelihood estimation within LOADEST. Daily values were aggregated on an annual basis for comparison with WEPP-simulated sediment yields.

Silt fences are considered among the most effective methods to measure hillslope erosion (Robichaud and Brown, 2002; Ypsilantis, 2011). A 30-m silt fence of a synthetic geotextile fabric with mesh size 0.3 to 0.8 mm was installed across a steep (50% slope) clear-cut hillslope in WS 1 to document hillslope erosion rates. The installation took place during the summer of 2003, one year after timber harvest and three months after a broadcast burn of the clear-cut, following the protocols described by Robichaud and Brown (2002). The silt fence was checked monthly during snow-free periods. The upslope catchment area above the silt fence measured ~0.15 km^2.

2.3. Model application

A detailed description of the WEPP model and summary of important model components and functions can be found in the WEPP User Summary (Flanagan and Livingston, 1995), WEPP Technical Documentation (Flanagan and Nearing, 1995), and a special book chapter (Flanagan et al., 2001). A brief summary of the model description and its recent modifications for agricultural- and forestland applications are presented in Appendix A.

2.3.1. Modifications for ET changes during post-harvest vegetative recovery in WEPP

To mimic multispecies in WEPP, canopy characteristics are lumped and represented with effective parameters.*LAI* is a sensitive parameter for soil evaporation and plant transpiration (He et al., 2012; Schmaltz et al., 2018; Qu and Zhuang, 2018). In WEPP, daily *LAI* for perennial crops in WEPP is computed following an equation described in the Environmental Policy Integrated Climate (EPIC) model (Williams et al., 1983), which is a function of maximum potential *LAI* (LAI_{mx}) and daily above-ground live biomass:

$$LAI = \frac{LAI_{mx}B_m}{B_m + 0.276e^{-13.6B_m}} \tag{1}$$

where LAI_{mx} is maximum leaf area index (m^2 m^{-2}), and B_m is above-ground live biomass (kg m^{-2}).

The relationship between *LAI* and B_m was derived for alfalfa and bromegrass perennial crops from cropland field study data. This relationship is inadequate for representing forest regrowth. We modified WEPP in this study assuming that *LAI* is simply a linear function of canopy cover such that when canopy cover reaches 100%, *LAI* reaches LAI_{mx} given by

$$LAI = LAI_{mx}C_c \tag{2}$$

where C_c is percent canopy cover.

Plant-specific parameters, including the canopy cover coefficient, canopy height coefficient, biomass energy ratio, fraction of canopy cover and biomass remaining after senescence, maximum canopy height, maximum *LAI*, and maximum rooting depth, can be adjusted in the WEPP management file to describe above-ground live biomass, percent canopy cover, canopy height, and live root mass for field conditions (Arnold et al., 1995).

2.3.2. Simulation methods

2.3.2.1. Model setup and parametrization. WEPP requires four main input files to describe topography, climate, soil characteristics, and management (Flanagan and Livingston, 1995). The Online GIS WEPP interface (http://milford.nserl.purdue.edu/ol/wepp/wepp1.php) (Frankenberger et al., 2011) was used to delineate the watershed structure for each watershed. The interface uses the TOPAZ (Topographic Parameterization; Garbrecht and Martz, 1999) tool and the USGS National Elevation Dataset (NED) 30-m DEM (Digital Elevation Model) for watershed delineation with the default values of 60 m for the minimum source channel length (MSCL) and 4 ha for the critical source area (CSA). The hillslope and channel configurations for each delineated watershed are presented in Table B1. Individual WEPP climate input files were created for the centroid of each hillslope from January 1990, to December 2007, using the 1000-m resolution DAYMET gridded datasets (Thornton et al., 2014) of daily precipitation, maximum and minimum temperatures, solar radiation, and dew-point temperature. Additional WEPP climate inputs that describe precipitation characteristics (event duration, normalized peak intensity, and time to peak intensity), and wind speed and direction were stochastically generated using CLIGEN *v*5.3 (Nicks et al., 1995), based on the monthly statistics of the long-term historical weather data from the NCDC weather station at Saint Maries, Idaho, 27 km northwest of the MCEW.

Major soil inputs for hillslopes are shown in Table B2. The soil file was built in a special, WEPP 7778 format, which allows the specification of effective hydraulic conductivity, field capacity, wilting point, and anisotropy ratio for each soil layer (Brooks et al., 2016). Soil textural properties for Bouldercreek soils were obtained from SSURGO (USDA NRCS, 2014). Baseline rill- and interrill erodibilities and critical shear stress were determined from the forest soil erodibility values used with the online Disturbed WEPP interface (Elliot, 2004). Anisotropy ratio, the relative predominance of lateral versus vertical permeability, was set to 15 for the top two soil layers to represent preferential flow through the lateral root systems (Srivastava et al., 2013; Brooks et al., 2016). The saturated hydraulic conductivity (K_{sat}) of a restrictive bedrock layer at the bottom of the soil profile was set to 0.02 mm h^{-1} for granitic rocks (Srivastava et al., 2013, 2017).

Management inputs for pre-treatment (undisturbed) and post-treatment (clear-cut and partial-cut) conditions are shown in Table B3. For the simulation period of 1992–2007, three separate management files were created for three management scenarios:

(1) undisturbed forest, (2) undisturbed forest followed by a partial-cut in August 2001, and (3) undisturbed forest followed by clear-cut and a low-severity burn in August 2001, and replanting in May 2003 (Fig. A1). The effects of road networks on the hydrology and erosion were not simulated as the current online WEPP interface does not have the capability to delineate road networks.

Vegetative parameters for each hillslope were derived from 30-m gridded data or literature values. Fig. A1 shows the daily above-ground biomass, average canopy cover, average canopy height, and *LAI* for all three scenarios for the entire simulation period. The 30-m gridded canopy cover and canopy height layer from the 2001 and 2010 Landfire data distribution website (http://landfire.cr.usgs.gov) were used to characterize average canopy cover and average canopy height for undisturbed and treated conditions. For pre- and post-treatment periods, *LAI* was determined using the relationship described in Eq. (2). Du et al. (2016) showed *LAI* ranging from 0 to less than 1 for clear-cut conditions, which corroborates well to that estimated in our study. Two parameters in the Penman-Monteith FAO *ET* model, the basal crop coefficient, k_{cb}, and depletion fraction, *p*, for coniferous trees, were set to 0.95 and 0.70, respectively, following Allen et al. (1998) (Table B3). The maximum rooting depth for undisturbed forest and partial-cut conditions was set to 1.2 m based on SSURGO data (USDA NRCS, 2014), and it was assumed to be 0.5 m for understory cover following clear-cut and after replanting. For undisturbed and partial-cut conditions, 100% cover was assumed, while for clear-cut and low-severity burn conditions, simulations were initiated with 80% cover (Robichaud, 2000; Elliot, 2004). The baseflow coefficient (k_b) of 0.02 d^{-1} was obtained from the recession curve of observed streamflow data for 1992–2007 (Sánchez-Murillo et al., 2014). A "naturally eroded channel" shape with "waterway with a gravel base" channel management was used to represent channels. The associated WEPP default parameter values are presented in Table B4. The channel critical shear stress was the only parameter used to calibrate channel sediment transport.

2.3.2.2. WEPP simulations. For this study, we incorporated a baseflow component directly into the WEPP model (*v*2012.8) that allocates baseflow from hillslopes into, and then route it through the channel networks. This version of WEPP with added baseflow function is available at the University of Idaho's online WEPP interfaces (https://wepp1.nkn.uidaho.edu/weppcloud/).

Continuous daily WEPP simulations were performed for all seven watersheds for 1990–2007. We conducted streamflow simulations without calibration following Brooks et al. (2016). For sediment yield, we calibrated the model for 1992–1997 (pre-treatment years) and evaluated the model performance for 1998–2007 (post-treatment years). We used the model-independent nonlinear parameter estimation package PEST (Doherty, 2005) in combination with WEPP to minimize the least-square error between observed and simulated annual sediment yields at the outlet of each watershed.

Simulated snow-water equivalent was compared to the observed at the Mica Creek SNOTEL station. Simulated soil-water content and plant transpiration were compared with the field-observed values in WS 3. Comparison between point-scale field-observed data and hillslope-scale WEPP-simulated values is presented in Appendix B.

2.3.2.3. Model evaluation statistical criteria. WEPP model performance was assessed using the Nash-Sutcliffe Efficiency (*NSE*; Nash and Sutcliffe, 1970), the Kling-Gupta efficiency (Gupta et al., 2009), and the deviation of runoff volume (D_v; Moriasi et al., 2007). *NSE* and *KGE* ranges from $-\infty$ to 1. A value of one indicates a perfect fit between simulated and observed data whereas a value of zero suggests that the model results are no better than the mean of the observed value. A negative value indicates that the observed mean value is better than the model predictions. D_v indicates the overall bias in the model (Gupta et al., 1999). Positive values signify model under-prediction and negative values over-prediction.

2.3.2.4. Analysis of treatment effects on water and sediment yield. The effect of timber harvest on annual (water year, October–September) water and sediment yield was evaluated by comparing reference and treated watersheds using analysis of covariance (ANCOVA) following Hubbart et al. (2007a). Separate regression analysis was performed to evaluate the ability of WEPP to simulate timber harvest effects relative to the observed data for pre-treatment (1992–1996), post-road (1997–2001), and post-harvest (2002–2007) periods (Stednick, 1996). A linear regression relationship was first established between the paired watersheds (reference and treated) for the pre-treatment period using annual water and sediment yields. The regression slope for the pre-treatment was then used for a new regression fit between the water and sediment yields from the reference and treated watersheds to determine the *y*-axis intercepts for post-road and post-harvest treatment periods. Changes in water and sediment yields were computed as a difference of the intercept values between the pre-treatment, post-road, and post-harvest treatments.

3. Results and discussion

3.1. Assessment of undisturbed reference watershed (WS 3)

3.1.1. Streamflow

There was a good overall agreement between simulated and observed annual streamflow from the undisturbed reference watershed with an average *NSE* of 0.67, *KGE* of 0.77, and D_v of −3% across all water years (Table B5). The *NSE* and *KGE* for specific years ranged from 0.43 to 0.78, 0.29 to 0.87, and D_v varied from −34% to 15% (Table B5). Between 1992 and 2007 the study site experienced substantial variation in annual precipitation, ranging from a minimum 863 mm in 1994 to a maximum of 1950 mm in 1997 with an annual average amount of 1337 mm during the 16-yr period. Simulated average water yield similarly varied from a minimum of 252 mm in 1994 to a maximum of 957 mm in 1997, averaging 541 mm yr^{-1} (Table B5) and accounting for 40% of mean annual precipitation.

WEPP-simulated streamflow captured the general trend of the observed hydrograph from the undisturbed reference watershed (WS 3) throughout the simulation period (Fig. 2). However, WEPP under-predicted the streamflow peaks for most years except 1993, 1997, and 2002, when the peaks were over-predicted. The over-predicted peaks were due to saturation-excess runoff resulting from snowmelt in May when the total soil water exceeded 650 mm in the 1520 mm soil profile (or, an average soil–water content of 0.43 m^3 m^{-3}). The observed streamflow recession during summer months (July–September) was well represented by WEPP in all years. However, WEPP missed some of the small peaks during the early precipitation events in October–November. This may be due to the difficulties in determining whether precipitation occurring when temperatures fluctuate around 0° C is rain, snow, or a mix of the two (Srivastava et al., 2017) and in simulating early season snowmelt.

3.1.2. Water balance

The incorporation of baseflow component in WEPP allowed to evaluate complete water balance for our study watersheds. The WEPP simulations suggest that water movement within the undisturbed WS 3 is dominated by subsurface lateral flow and baseflow

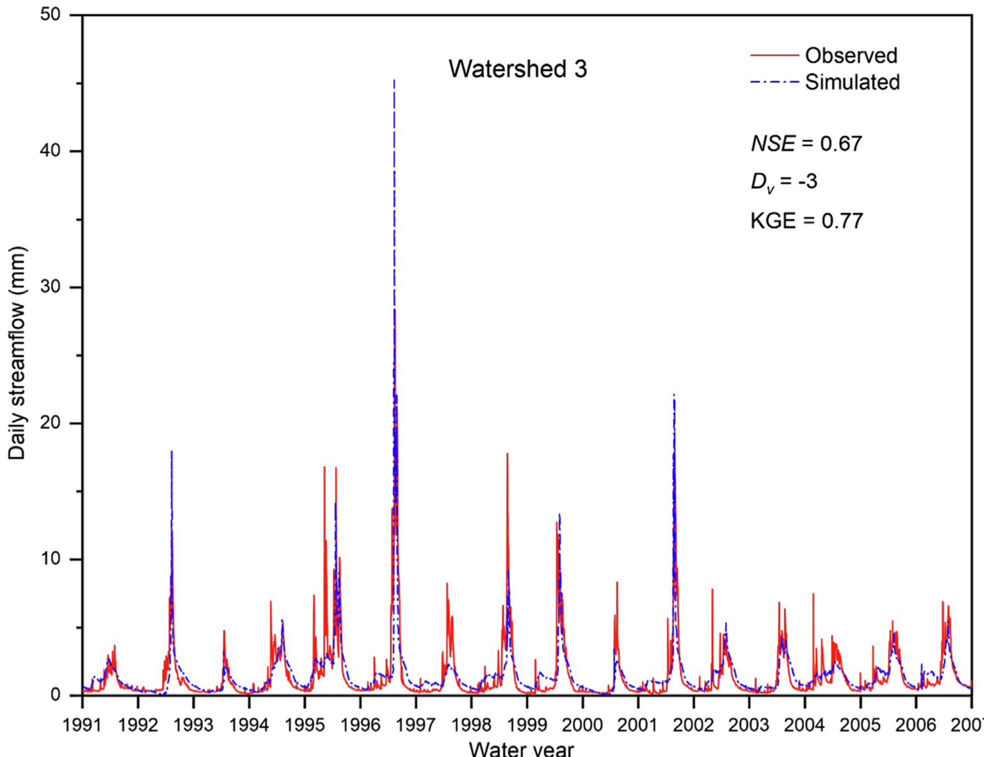

NSE	0.51	0.65	0.54	0.66	0.55	0.74	0.43	0.54	0.50	0.61	0.78	0.49	0.70	0.51	0.72	0.67
KGE	0.61	0.71	0.53	0.74	0.63	0.87	0.29	0.47	0.62	0.54	0.85	0.61	0.70	0.45	0.69	0.63
Dv	-34	15	-13	-6	2	-1	6	7	-13	6	-7	-32	-14	-1	-4	1

Fig. 2. Comparison of observed and WEPP-simulated daily streamflow for WS 3 from 1992 to 2007.

with minimal surface runoff (Table B5). For the 16-year period, simulated surface runoff, subsurface lateral flow, and baseflow from hillslopes account for 1%, 28%, and 12% of precipitation, respectively. This insignificant amount of surface runoff is typical of undisturbed forest soils with thick duff layers and high infiltration capacities (Elliot et al., 2016). The peak discharge during the snowmelt season was primarily from subsurface lateral flow from upland hillslopes. The surface runoff, subsurface lateral flow, and baseflow contributions to simulated streamflow were 3%, 68%, and 29%, respectively.

The change in total soil water and groundwater storage from one year to the next on October 1st averaged 0.7 mm and zero mm, respectively, for the entire 16 years. WEPP-simulated annual *ET* varied from 655 mm to 944 mm with an average of 795 mm (59% of mean annual precipitation).

3.2. Assessment of all watersheds

3.2.1. Streamflow

WEPP's ability to simulate streamflow for the disturbed watersheds (WS 1, 2, 4, and 7) was similar to that for the undisturbed watersheds (WS 3, 5 and 6) as demonstrated by the *NSE*, *KGE*, and D_v values for all the seven watersheds for both the entire simulation period and individual treatment periods (Table 1). The overall *NSE*, *KGE*, and D_v ranged from 0.58 to 0.71, 0.67 to 0.81, and −3 to 9%, respectively, suggesting "satisfactory" to "good" model performance according to the statistical model performance evaluation criteria submitted by Moriasi et al. (2007), Ritter and Muñoz-Carpena (2013) and Gupta et al. (2009). The overall ability of WEPP to achieve this level of agreement with observed data using an uncalibrated hydrology model is noteworthy.

During the pre-treatment period (1992–1997), the *NSE* for the seven watersheds varied from 0.57 to 0.75, the *KGE* from 0.73 to 0.88, and D_v ranged from −2 to 8%. The *NSE* and *KGE* values for the post-road treatment period (1998–2001) ranging from 0.49 to 0.60 and from 0.45 to 0.66, respectively, were lower compared to pre- and post-harvest treatment periods. These lower *NSE* and *KGE* values are likely due to under-prediction of the streamflow peaks as *NSE* and *KGE* are sensitive to peak values (see Fig. 2). For the post-road treatment period, the positive D_v values suggest under-prediction of simulated streamflow by 9% to 19% for all watersheds except WS 3 with a much smaller, 1% under-prediction. Over the post-harvest treatment period of 2002–2007, *NSE* and *KGE* ranged from 0.55 to 0.73 and 0.56 to 0.77, respectively, with the lowest *NSE* and *KGE* for WS 1, which underwent clear-cut treatment. D_v values during this period ranged from −8% to 10%. The agreement between the WEPP-simulated and observed streamflow is similar to that achieved by the DHSVM model applied to the same watersheds (Du et al., 2013). In that study, DHSVM was run at a 3-hr time step to calibrate streamflow against observed data for 1993–2007. The resulting *NSE* and D_v values for WS 1–7 ranged from 0.69 to 0.79 and −1.5 to 12.3%, respectively.

3.2.2. Water balance

The simulated annual water balance for watersheds 1–7 separated into pre-treatment, post-road treatment, and post-harvest treatment periods is shown in Table 2. The major components of the water balance presented are precipitation, *ET*, surface runoff, subsurface lateral flow, and baseflow. The effect of timber harvest treatment on the hydrologic regime in the MCEW varied with the location and size of the watershed, the type of treatment, and the time since treatment.

For the pre-treatment period of 1992–1997, simulated water yield for the seven watersheds ranged from 557 mm to 606 mm and precipitation varied from 1340 mm to 1418 mm. A major por-

Table 1
NSE, *KGE*, and D_v of observed and WEPP-simulated daily streamflow for pre-treatment, post-road treatment, and post-harvest treatment periods.

Watersheds	Statistical Criteria	Pre-treatment (1992–1997)	Post-road treatment (1998–2001)	Post-harvest treatment (2002–2007)	Overall (1992–2007)
1	*NSE*	0.74	0.54	0.55	0.63
	KGE	0.84	0.45	0.56	0.67
	D_v	7	19	6	9
2	*NSE*	0.75	0.6	0.72	0.71
	KGE	0.88	0.66	0.71	0.81
	D_v	1	14	6	6
3	*NSE*	0.71	0.53	0.72	0.67
	KGE	0.88	0.54	0.77	0.77
	D_v	−2	1	−8	−4
4	*NSE*	0.75	0.57	0.73	0.71
	KGE	0.84	0.53	0.62	0.72
	D_v	3	16	10	9
5	*NSE*	0.59	0.49	0.62	0.58
	KGE	0.75	0.46	0.65	0.68
	D_v	4	18	−1	6
6	*NSE*	0.57	0.57	0.66	0.59
	KGE	0.73	0.54	0.72	0.71
	D_v	8	15	−3	6
7	*NSE*	0.62	0.59	0.69	0.63
	KGE	0.80	0.57	0.64	0.74
	D_v	0	9	−8	−1

[†]Watersheds 3, 5, and 6 were kept undisturbed for the entire simulation period.

Table 2
WEPP-simulated major water balance components. All fluxes are computed water-year wise.

Watershed	P*	ET	E_p	E_s	Q_{surf}	Q_{lat}	Q_b	Q_{sim}	Q_{obs}+	$EST\ ET$#
	mm yr^{-1}									
Pre-treatment period (1992–1997)										
1	1376	790 (57)	743	48	16 [3]	419 [72]	145 [25]	579 (42)	619 (45)	757 (58)
2	1418	805 (57)	758	47	21 [4]	440 [73]	145 [24]	606 (43)	609 (43)	809 (59)
3	1405	820 (58)	774	46	25 [4]	402 [70]	152 [26]	578 (41)	565 (40)	840 (62)
4	1395	802 (57)	755	47	4 [1]	435 [74]	148 [25]	586 (42)	607 (43)	788 (59)
5	1334	759 (57)	709	51	2 [0]	426 [75]	142 [25]	567 (43)	591 (44)	743 (58)
6	1340	767 (57)	716	50	1 [0]	424 [75]	142 [25]	566 (42)	618 (46)	722 (57)
7	1345	781 (58)	732	49	2 [0]	411 [74]	146 [26]	557 (41)	557 (41)	788 (61)
Post-road treatment period (1998–2001)										
1	1243	774 (62)	729	45	2 [0]	328 [69]	150 [31]	479 (39)	594 (48)	648 (53)
2	1284	792 (62)	748	44	8 [2]	344 [68]	151 [30]	502 (39)	583 (45)	701 (55)
3	1271	812 (64)	771	42	4 [1]	313 [66]	156 [33]	472 (37)	475 (37)	796 (63)
4	1261	790 (63)	746	44	3 [1]	328 [68]	152 [32]	482 (38)	576 (34)	685 (56)
5	1279	743 (62)	696	46	0 [0]	325 [70]	143 [31]	467 (39)	566 (47)	630 (54)
6	1200	749 (63)	703	46	1 [0]	321 [69]	144 [31]	465 (39)	549 (46)	651 (56)
7	1209	763 (63)	718	45	1 [0]	311 [68]	149 [32]	459 (38)	506 (42)	703 (59)
Post-harvest treatment period (2002–2007)										
1	1285	503 (40)	401	102	13 [1]	595 [77]	168 [22]	771 (60)	823 (64)	462 (35)
2	1329	670 (51)	596	74	12 [1]	477 [73]	168 [26]	652 (49)	692 (52)	637 (47)
3	1312	758 (58)	721	38	9 [1]	375 [68]	169 [31]	549 (42)	508 (39)	804 (61)
4	1304	669 (52)	605	64	2 [0]	462 [73]	167 [27]	627 (48)	697 (53)	606 (46)
5	1196	699 (57)	656	43	2 [0]	381 [71]	156 [29]	534 (43)	530 (43)	708 (57)
6	1240	705 (57)	663	42	2 [0]	375 [70]	158 [30]	528 (43)	514 (41)	726 (58)
7	1249	685 (55)	632	53	2 [0]	398 [71]	163 [29]	557 (45)	517 (41)	732 (58)

Parenthesis (): values as percentage of P.
Brackets []: values as percentage of Q_{sim}.
* P, precipitation;, ET, evapotranspiration;, E_p, plant transpiration, E_s; soil evaporation, Q_{surf}, surface runoff; Q_{lat}, subsurface lateral flow; and Q_b, baseflow from groundwater storage. The sum of Q_{surf}, Q_{lat}, and Q_b forms the simulated water yield, Q_{sim}.
\+ Q_{obs} is observed water yield to compare with Q_{sim}.
\# $EST\ ET$ is estimated ET using water balance (=$P_{\mathrm{DAYMET}} - Q_{obs}$). Percent ET shown in brackets was calculated as $EST\ ET$ over P_{DAYMET}.

tion of water was lost as *ET* ranging from 759 to 820 mm and averaging 57% of annual precipitation. Subsurface lateral flow and baseflow were in the range of 402–440 mm and 142–152 mm, respectively. During the post-road treatment period of 1998–2001, precipitation ranged 1200–1284 mm, and the simulated water yield varied from 459 mm to 502 mm. Simulated annual *ET* during this period was 743–812 mm, comparable with the *ET* range during the pre-treatment period. However, subsurface lateral flow during the post-road period decreased, and baseflow increased as compared to those during pre-treatment years with higher precipitation.

For the post-harvest period of 2002–2007, WEPP results reflect the hydrologic impact of forest clear-cut (WS 1) and partial-cut (WS 2) on *ET*, subsurface lateral flow, and water yield. The decrease in *ET* in WS 1 and WS 2 resulted in an overall increase in both subsurface lateral flow and water yield. For WS 1 and WS 2, the subsurface lateral flow contributions to streamflow were 77% and 73%, respectively, compared to 68% for the undisturbed WS 3.

Several researchers have applied hydrologic models to the MCEW to simulate hydrologic processes (e.g., Chen et al., 2005; Du et al., 2013); however, they did not report the effect of timber harvest on watershed *ET*. We compared WEPP-simulated *ET* to that estimated using a watershed water balance approach (EST *ET*), defined as the residual of average annual precipitation and discharge. This approach is reasonable as the MCEW is underlain by a bedrock of low permeability (Chen et al., 2005). Comparison of WEPP-simulated annual *ET* and EST *ET* for WS 1–7 during pre-, post-road, and post-harvest treatment periods shows a good agreement overall (Table 2). For the pre-treatment period, WEPP-simulated *ET* comprised 57–58%, while EST *ET* 57–62%, of annual precipitation over different watersheds (Table 2). For the post-road period, WEPP-simulated *ET* was slightly higher (62–63% of annual precipitation) than those of EST *ET* (54–63% of annual precipitation), which may be due to the under-prediction of peak flows that would have left the watershed during spring snowmelt rather than recharging the root zone and later lost to *ET*. For the post-harvest period, WEPP-simulated and EST *ET* were compatible, ranging 40–58% and 35–61% of annual precipitation, respectively.

3.2.3. Treatment effects on water yield

The effects of timber harvest on water yield were represented reasonably well by WEPP based on the ANCOVA regression. Comparison of observed and WEPP-simulated mean annual water yield and its relative changes from pre- to post-road and post-harvest treatments for all paired watersheds using ANCOVA (Table 3). Figs. B2 and B3 show the comparison of observed and simulated trends of annual water yield for paired watersheds (treated vs. reference) during pre-treatment, post-road, and post-harvest periods using the regression analysis.

3.2.3.1. Post-road treatment effects. Road construction in 1997 in WS 1 with the clear-cut treatment resulted in a statistically significant ($p < 0.05$) increase in observed water yield of 76 mm yr^{-1} or 12% (Table 3, Fig. B2a). For WS 2, there was an increase in observed water yield of 65 mm yr^{-1} or 11% (Fig. B2c) following road construction with a partial-cut treatment, the increase was not statistically significant (p-value = 0.063). Increases in observed water yield at the outlet of WS 4 and WS 7, too, were not statistically significant during the road treatment as suggested by p-values (>0.05) (Table 3, Fig. B3a, c) suggesting that the impact on water yield increase at WS 4 or downstream at WS 7 was considerably dampened at these larger spatial scales.

As road features were not simulated in WEPP, there were no significant differences in simulated water yield between treated (WS 1 and WS 2) and undisturbed (WS 3) watersheds during the post-road period. The simulated water yield increase from WS 1 (8 mm yr^{-1} or 1%) (Table 3, Fig. B2b) and WS 2 (7 mm yr^{-1} or 1%) (Table 3, Fig. B2d) were not statistically significant (p-value > 0.05) compared to water yield from the reference WS 3. Although roads cover only a small fraction of the land surface, many studies have documented greater runoff from watersheds with roads compared to watersheds without roads (Gucinski et al., 2001; Jones and Grant, 1996; Grace, 2017). The compact impervious road surfaces generate runoff even during small storms, the lack of vegetation on roads reduces *ET*, and in some cases, the road cutslope incision intercepts subsurface flow and

Table 3
Regression analysis of observed and WEPP-simulated annual water yield (water year) at the Mica Creek Experimental Watershed (MCEW) during the pre-treatment, post-road treatment, and post-harvest treatment periods.

Watershed comparison	Time Period	Reference(mean water yield, mm)	Treatment(mean water yield, mm)	Intercept (mm)	Intercept p-value	Change in water yield (mm)	Percentage change
Observed							
WS 3/WS 1	A	565	619	−16	–	–	–
	B	475	594	61	0.002	76	12
	C	508	823	268	0.000	284	34
WS 3/WS 2	A	565	609	38	–	–	–
	B	475	538	103	0.063	65	11
	C	508	692	199	0.000	161	23
WS 5/WS 4	A	591	607	22	–	–	–
	B	566	576	15	0.862	−7	−1
	C	530	697	152	0.000	130	19
WS 6/WS 7	A	618	557	4	–	–	–
	B	549	506	14	0.495	10	2
	C	514	517	52	0.014	48	9
WEPP-simulated							
WS 3/WS 1	A	578	579	−7	–	–	–
	B	472	479	1	0.127	8	1
	C	549	771	216	0.000	223	29
WS 3/WS 2	A	578	606	0	–	–	–
	B	472	502	7	0.146	7	1
	C	549	652	72	0.000	72	11
WS 5/WS 4	A	567	586	12	–	–	–
	B	467	482	10	0.856	−2	0
	C	534	627	87	0.000	75	12
WS 6/WS 7	A	566	557	11	–	–	–
	B	465	459	9	0.797	−1	0
	C	528	557	50	0.000	39	7

Time period A is pre-treatment (1992–1997), B is post-road treatment (1998–2001), and C is post-harvest treatment (1998–2001); WS are watersheds. Intercepts are significantly different at p-value < 0.05. WS 3 is a reference watershed for the treated WS 1 and 2. WS 5 is a reference watershed for the treated WS 4 encompassing WS 1, 2, and 3. WS 6 is a reference watershed for the treated WS 7 encompassing WS 1, 2, 3, and 4.

diverts it to surface runoff, rather than allowing the subsurface lateral flow to remain in the soil profile to support late-season *ET* (Luce and Wemple, 2001; Bachmair and Weiler, 2011). Increases in simulated water yield for WS 4 and WS 7 (Table 3, Fig. B2b, d) were also not statistically significant (p-value > 0.05), agreeable with the observed data.

3.2.3.2. Post-harvest treatment effects. Observed and WEPP-simulated annual water yield for the post-harvest period increased significantly in all watersheds with p values less than 0.05 (Table 3). Increase in observed water yield was 284 mm yr^{-1} (34%) at WS 1 due to clear-cut and was 161 mm yr^{-1} (23%) at WS 2 due to partial-cut (Table 3, Fig. B2a, c). WEPP-simulated increase in water yield at WS 1 (223 mm yr^{-1} or 29%) and WS 2 (72 mm yr^{-1} or 11%) were lower than those observed (Fig. B2b, d). Observed water yield from WS 4 (paired with WS 5 and including watersheds 1, 2, and 3) increased by 130 mm yr^{-1} (19%) (Table 3, Fig. B3a) whereas simulated water yield increased by 75 mm yr^{-1} (12%) (Table 3, Fig. B3b). Both simulated and observed water yields represent a statistically significant increase at WS 7 (paired with WS 6 and including watersheds 1, 2, 3, and 4) of 39 mm yr^{-1} (7%) and 48 mm yr^{-1} (9%), respectively (Table 3, Fig. B3c, d).

The under-prediction of the water yield by WEPP could be due to the complex dynamics of vegetative growth both spatially and temporally. We used a simple linear relationship (Eq. (2)) to derive *LAI* from simulated canopy cover because of lack of known relationship between *LAI* and above-ground live biomass with age. Understanding the relationships between *LAI* and above-ground live biomass for forest stands of different species and ages and incorporating them into WEPP will likely improve the model's ability to adequately simulate water yield.

3.2.4. Sediment yield

Observed data indicated that the road construction, clear cutting, and partial cutting operations resulted in increased sediment yield at the downstream watershed outlets with the predominant source of sediment being instream erosion with little to no contributions from upland hillslope erosion. Despite substantial clear-cut operations in WS 1, no major rill or gully erosion was observed in any of the watersheds throughout the study. The 30 m silt fence installed on a 50% slope in the clear-cut WS 1 did not catch any sediment from 2003 to 2005. WEPP did not predict any erosion from these disturbed hillslopes during the entire simulation period of 1992 to 2007 likely due to higher hydraulic conductivity of the soil surface layer. Post-harvest in situ observations noted no evidence of hillslope erosion contribution to the silt fence. Similarly, a nearby study did not measure any soil movement from hillslopes disturbed with timber harvest and prescribed fire during the same time period (Elliot and Glaza, 2008). Since our study was designed and supported by a private timber company to assess the downstream impacts of timber harvest practices on water quality, care was taken to ensure good forestry management practices were implemented in the study. For example, most roads in WS 1 and 2 were outsloped to ensure short overland flow lengths and minimize the risk of erosion. In locations where insloped ditches were present, BMPs, such as ditch relief culverts, filter windrows, straw bales near stream crossings, and spot-rocked roads, were implemented to minimize delivery of sediment to streams (Barkley et al., 2015). As a result, there was little observed road erosion and or evidence that this erosion provided a significant amount of sediment to the streams. Hence, the predominant sources of increased sediment in the watersheds were instream. Following the common descriptor of stream bed particle-size distribution that identifies the percent particles below a critical diameter threshold (e.g. 25% of the particles in a stream bed have diameters finer than the D25 particle-size diameter) and a classification that gravel-bed streams have a D50 particle size ranging 2–64 mm and cobble-bed streams have D50 particle diameters>64 mm, we concluded that WS 7 is a cobble-bed stream and WS 1–6 are all gravel-bed streams as indicated by Fig. 3a, which shows the comparison of watershed-wide observed D25, D50, and D80 bed particle sizes obtained from cumulative particle-size distribution analysis of pebble count data, and the calibrated channel critical shear stress. The overall trend and magnitude of the calibrated critical shear stress for each watershed match well with D50 particle size trends: the greater the particle size the greater the calibrated critical shear stress. D50 particle size varied from 18 mm in WS 5 to 65 mm in WS 7 (Fig. 3a). The calibrated critical shear stress val-

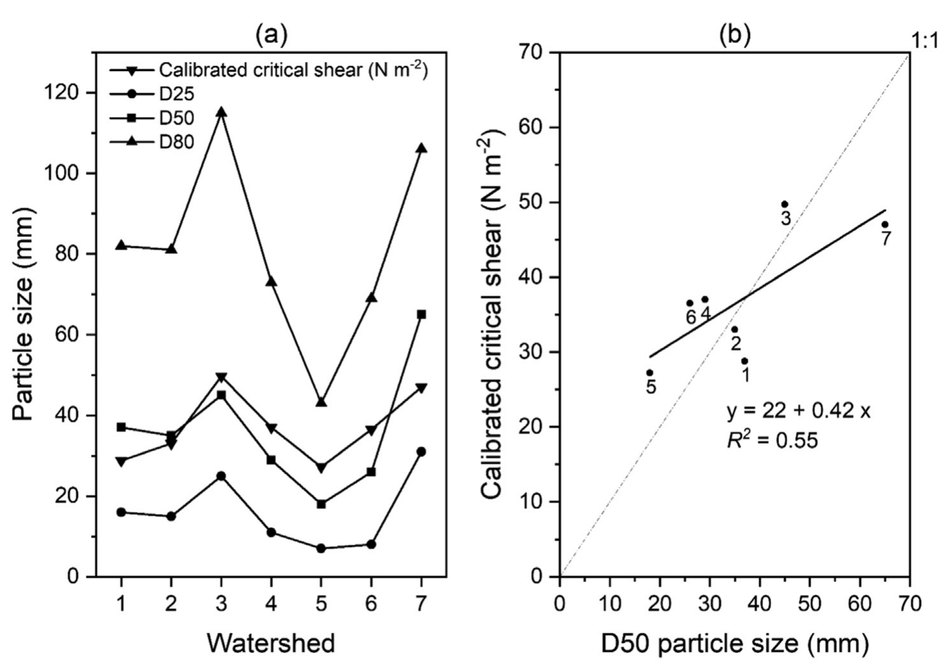

Fig. 3. Comparison of (a) watershed-wise observed D25, D50, and D80 bedload particle size to calibrated critical shear stress and (b) D50 particle size and calibrated critical shear stress on a scatterplot.

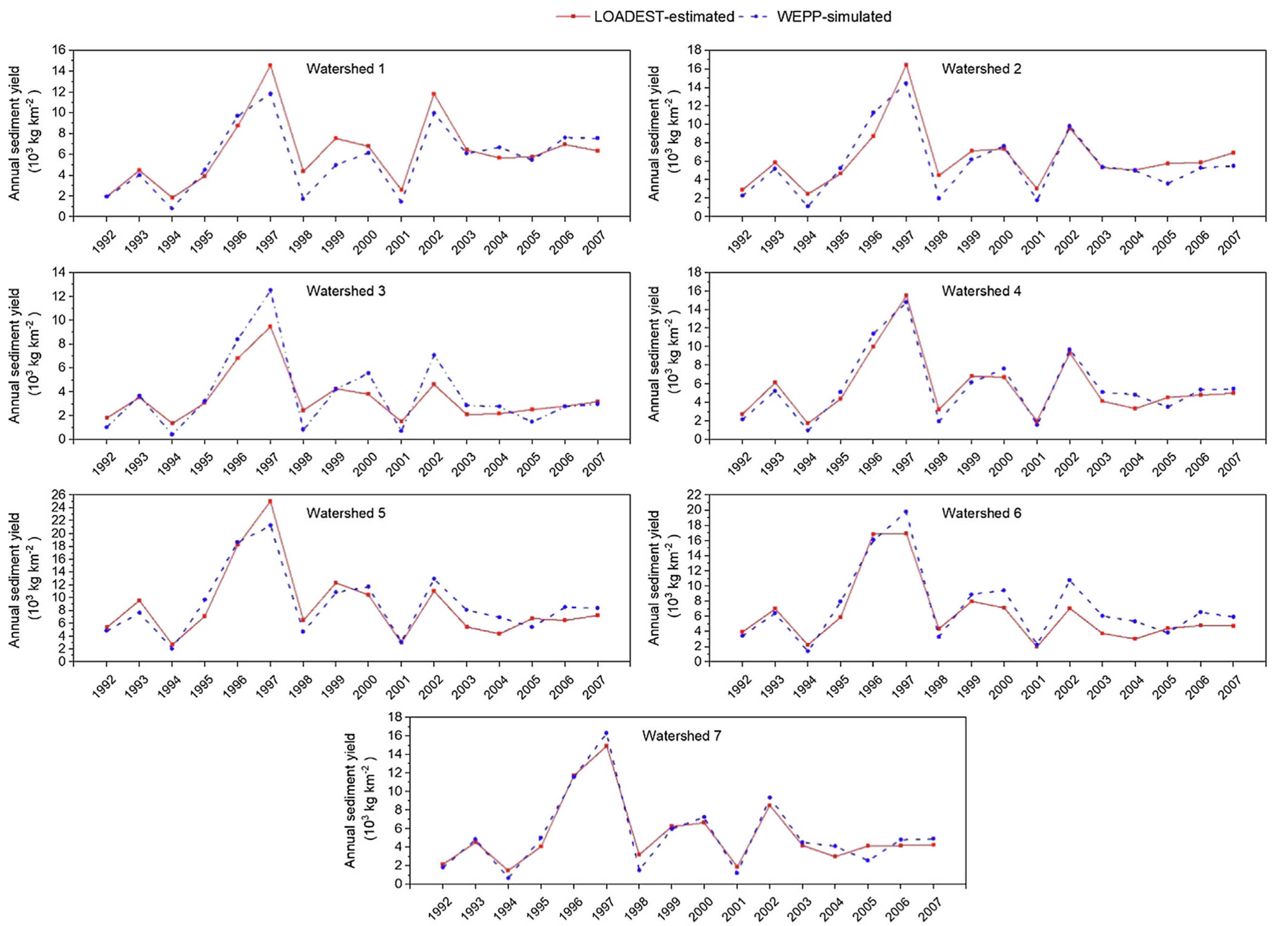

Fig. 4. Comparison of LOADEST-estimated observed and WEPP-simulated annual sediment yields for watersheds 1–7 from 1992 to 2007 (calibration period: 1992–1997, performance assessment period: 1998–2007).

ues ranged from a minimum of 29 N m^{-2} in WS 1 to a maximum of 50 N m^{-2} in WS 3. Interestingly, the undisturbed reference stream in WS 3 had the largest particle size of all gravel-bed streams in the MCEW and would be considered a coarse gravel-bed stream. The direct relationship between calibrated critical shear stress and the D50 particle size suggests that it is possible to estimate critical shear stress from pebble count data in applying WEPP to ungauged basins as shown in Fig. 3.

Sediment transport for a given particle size occurs when the hydraulic shear stress exceeds the critical shear stress. Berenbrock and Tranmer (2008) estimated critical shear stress values of different bedload particle sizes measured at several gauging stations within the Coeur d'Alene River Basin north of the MCEW. Estimated critical shear stress varied from 12 N m^{-2} to 26 N m^{-2} for particle diameters ranging 16–32 mm. For particle diameters between 32 mm and 64 mm, the estimated critical shear stress varied from 26 N m^{-2} to 54 N m^{-2}. Our calibrated critical shear stress values were in the same range as those estimated by Berenbrock and Tranmer (2008).

Fig. 4 shows the comparison of LOADEST-estimated and WEPP-simulated annual sediment yields for 1992–2007 for watersheds 1–7. Table 4 summarizes the *NSE*, *KGE*, and D_v for the periods of pre-treatment calibration period and post-treatment model performance assessment. WEPP captured the trends of the observed annual sediment yield in both wet, high-snowmelt years (e.g. 2002) and drier, low-flow years (e.g. 2000). *NSE* and *KGE* ranging 0.62–0.97 and 0.43–0.97, respectively, for the calibration period and 0.61–0.95 and 0.42–0.97, respectively, for the model performance assessment period indicate good to very good agreement. D_v for the calibration period varied from −2 to + 2%, suggesting slight over- or under-prediction. For the model performance assessment period, D_v ranged from −24 to + 13%, indicating greater over- or under-prediction, but within acceptable ranges (Moriasi et al., 2007).

3.2.5. Treatment effects on sediment yield

WEPP successfully characterized the temporal changes in sediment yield with treatments based on the ANCOVA regression of the sediment yield data. Table 5 summarizes the comparison of observed and WEPP-simulated mean annual sediment yield and relative changes in sediment yield from pre- to post-road and post-harvest periods for all paired watersheds. Figs. B4 and B5 present the comparison of observed and simulated trends of annual sediment yield for the paired watersheds (treated vs. reference) during pre-treatment, post-road treatment, and post-harvest treatment obtained from the regression analysis.

3.2.5.1. Post-road treatment effects. There was a statistically significant increase in observed annual sediment yield of 1.55×10^3 kg m^{-2} (26%) in WS 1 after road construction in 1997 ($p < 0.05$) as shown in Table 5 and Fig. B4a. No significant differences in observed sediment yields were found in WS 2, WS 4, and WS 7 after road construction ($p > 0.05$) (Table 5, Figs. B4b and B5a, c). WEPP did not reproduce the significant increase in sediment yield

Table 4
NSE, *KGE*, and D_v of LOADEST-estimated observed and WEPP-simulated annual sediment yields for calibration and model performance assessment periods.

Watershed	Calibration (1992–1997)			Model Performance Assessment (1998–2007)		
	NSE	*KGE*	D_v	*NSE*	*KGE*	D_v
1	0.92	0.78	0	0.82	0.83	+12
2	0.62	0.43	−2	0.89	0.86	+13
3	0.78	0.54	−1	0.61	0.42	−12
4	0.90	0.76	+1	0.95	0.97	−1
5	0.92	0.92	0	0.90	0.81	−3
6	0.95	0.97	+2	0.77	0.68	−24
7	0.97	0.96	+1	0.93	0.82	−2

Table 5
Regression analysis of LOADEST-observed and WEPP-simulated annual sediment yield (water-year wise) at the Mica Creek Experimental Watershed (MCEW) during the pre-treatment, post-road treatment, and post-harvest treatment periods.

Watershed comparison	Time Period*	Reference (mean sediment yield, 10^3 kg km^{-2})	Treatment (mean sediment yield, 10^3 kg km^{-2})	Intercept (10^3 kg km^{-2})	Intercept *p*-value	Change in sediment yield (10^3 kg km^{-2})	Change in sediment yield (%)
Observed							
WS 3/WS 1	A	4.34	5.92	−1.1	–	–	–
	B	3.02	5.32	0.4	0.018	1.55	26
	C	2.91	7.16	2.4	0.000	3.57	50
WS 3/WS 2	A	4.34	6.85	−0.2	–	–	–
	B	3.02	5.51	0.6	0.156	0.80	12
	C	2.91	6.44	1.7	0.002	1.91	30
WS 5/WS 4	A	11.34	6.76	−0.2	–	–	–
	B	8.07	4.70	−0.3	0.945	−0.03	0
	C	6.87	5.20	1.0	0.015	1.20	23
WS 6/WS 7	A	8.80	6.48	−1.0	–	–	–
	B	5.36	4.50	−0.1	0.163	0.95	15
	C	4.61	4.71	0.8	0.011	1.81	38
WEPP-simulated							
WS 3/WS 1	A	4.88	5.47	1.0	–	–	–
	B	2.84	3.58	1.0	0.931	−0.04	−1
	C	3.32	7.23	4.2	0.000	3.17	44
WS 3/WS 2	A	4.88	6.61	1.1	–		–
	B	2.84	4.42	1.2	0.729	0.09	1
	C	3.32	5.78	2.1	0.002	0.91	16
WS 5/WS 4	A	10.69	6.62	−0.9	–		–
	B	7.58	4.33	−1.0	0.836	−0.08	−1
	C	8.38	5.67	−0.2	0.077	0.69	12
WS 6/WS 7	A	9.17	6.69	−1.0	–		–
	B	5.96	3.99	−1.0	0.964	−0.02	0
	C	6.42	5.05	−0.3	0.061	0.67	13

* Time period A is pre-treatment (1992–1997), B is post-road treatment (1998–2001), and C is post-harvest treatment (1998–2001); WS are watersheds. Intercepts are significantly different at *p*-value < 0.05. WS 3 is a reference watershed to treated WS 1 and 2. WS 5 is a reference watershed to treated WS 4 encompassing WS 1, 2, and 3. WS 6 is a reference watershed to treated WS 7 encompassing WS 1, 2, 3, and 4.

following road construction in WS 1 as road features were not simulated by the model (Figs. B4b, d and B5b, d). In a WEPP simulation study of road network erosion at the MCEW, Rackley and Chung (2008) simulated sediment yield of 1.0–6.4 Mg km^{-2}, depending on management scenario, suggesting that roads were likely contributing some sediment to the roaded watersheds, but the channel was likely the main source of sediment observed downstream.

3.2.5.2. Post-harvest treatment effects. For the post-harvest period, both observations and WEPP simulations indicated a significant increase in annual sediment yield in all treated watersheds with $p < 0.05$ (Table 5, Figs. B4 and A5). Observed sediment yield increased by 3.57×10^3 kg m^{-2} (50%) at WS 1 due to clear-cut and by 1.91×10^3 kg m^{-2} (30%) at WS 2 due to partial-cut. The WEPP-simulated increase in sediment yield was 3.17×10^3 kg m^{-2} or 44% for WS 1 and 0.91×10^3 kg m^{-2} or 16% for WS 2. There were significant increases in observed downstream sediment yields due to the harvest treatments: 1.20×10^3 kg m^{-2} (23%) at WS 4 and 1.81×10^3 kg m^{-2} (38%)) at WS 7. WEPP did not reproduce the statistically significant increases at the significance level of 0.05, though it did generate an increase in sediment yield of 0.69×10^3 kg m^{-2} (12%) for WS 4 and 0.67×10^3 kg m^{-2} (13%) for WS 7.

Karwan et al. (2007) evaluated the effects of treatment practices on sediment yields using data collected at the outlets of watersheds 1, 2, and 3 with WS 3 used as a reference. They found no significant impacts on sediment yields following road treatments at WS 1 and WS 2. A marginal increase in sediment yield was observed following the partial-cut in WS 2. A marked increase in sediment yield following the clear-cut in August 2001 in WS 1 was observed but only for a brief period immediately after harvest. A broadcast burn in May 2003 following the clear-cut did not result in a significant increase in sediment yield. The observation that prescribed burn had no major impact on sediment delivery was similar to that observed by Elliot and Glaza (2008). The authors inferred from their investigation that upland erosion from hillslopes following clear-cut and prescribed burn may not result in a significant increase in sediment yield, but that an increase in sediment yield is likely due to increased streamflow within the channel network itself, or from the reconstruction of the road network increasing runoff and therefore sediment generation.

3.3. Modeling limitations

Although in this study we demonstrated the applicability of WEPP as a modeling tool to simulate the effects of forest harvesting on water and sediment yield, we encountered several modeling limitations as presented below:

(a) Roads: Forest roads are the largest source of sediment generation from upland hillslope areas into streams (Luce and Black, 1999; Gomi et al., 2005). Soil compaction due to road construction restricts surface soil infiltration and can affect the magnitude and timing of peak flow (Wemple and Jones, 2003; Stednick and Troendle, 2016). Roads can intercept surface runoff and subsurface lateral flow from uplands, and rapidly deliver water and sediment into road ditches from where water and sediment is routed directly into stream channels (Wemple and Grant, 1996; Gomi et al., 2005; Hubbart et al., 2007a,b; Al-Chokhachy et al., 2016a, b). In our study, we modeled post-road treatment periods (1998–2001) without the inclusion of roads. Although a separate interface of WEPP is available for use to predict runoff and sediment generation from roads (Elliot, 2013; https://forest.moscowfsl.wsu.edu/cgi-bin/fswepp/wr/wepproad.pl), this interface has not been yet incorporated into the watershed version of WEPP.

(b) Plant growth: The increase in forest biomass during vegetative recovery often involves a change in species composition that includes unique canopy structures and growth rates (Yang et al., 2005; He et al., 2012). To adequately simulate such complex successional dynamics that includes multi-species interactions of over- and under-story canopy structures is challenging. In the current version of WEPP, simulating these multi-species dynamics is not possible due to a fundamental assumption that each OFE of a hillslope can only have one dominant vegetation type (Arnold et al., 1995). Furthermore, to properly represent *ET* through *LAI* and rooting depth, relationships between forest biomass and stand-age of different tree species is needed for use in WEPP.

(c) Soil heterogeneity: The spatial variability of soil texture, soil thickness and drainable porosity plays an important role in the generation of subsurface lateral flow, baseflow and saturation excess runoff and plant water uptake via *ET* (Bachmair and Weiler, 2011; Elliot et al., 2016) in steep forest hillslopes. For example, it is generally noticed that shallower soils are more common on the upland steeper slopes and deeper soils on the lowland gentler slopes of a hillslope (Elliot et al., 2016), which can affect drainable porosity and hydrological processes within the hillslope. In our study, we recognize the limitation of using a single soil series of uniform soil characteristics for the entire study area obtained from the publicly available SSURGO database.

4. Conclusions

The long-term paired and nested watershed study at the Mica Creek Experimental Watershed in northern Idaho, USA, with staged road construction and timber harvesting allowed for an assessment of the ability of the WEPP model to simulate the impacts of forest management practices on hydrologic regime, and, for the first time, sediment yield, from large forested watersheds in the Pacific Northwest, USA. WEPP was modified to better represent changes in *LAI* during post-harvest vegetative recovery. Additionally, a single parameter, the critical shear stress of stream bed, was calibrated to improve sediment yield simulation. In general, WEPP-simulated daily streamflow was in close agreement with the observed for all watersheds simulated, though WEPP tended to over-predict the streamflow for summer low-flow periods and under-predict the streamflow during the spring peak snowmelt period. WEPP could capture the changes in both water and sediment yield due to forest harvesting practices. We showed that, for gravel- and cobble stream beds, the critical shear stress was directly related to the median particle size based on a Wollman Pebble count. As such, estimation of this parameter could be based on easily measured physical properties in related future studies.

The ability of the WEPP model to reproduce the effects of forest harvesting practices on hydrologic regime (water yield, peak flow) and upland erosion and stream sediment transport with minimal calibration demonstrates WEPP's potential as a decision-aid tool for forest management in the Pacific Northwest of USA. Additionally, the online version of WEPP and the model's ability to draw on publicly accessible climatic, soil, and landuse databases enhances the ease of use and broad applicability of the model.

Future efforts should be devoted to establishing and incorporating the relationships between *LAI* and above-ground live biomass for different tree species and ages into WEPP. Evaluation of WEPP with species-specific stomatal resistance parameters in the Penman-Monteith method will help account for the effects of vapor pressure deficit on plant transpiration. The incorporation of road networks in the Online GIS WEPP interface will allow the assessment of changes in hydrology and sediment generation and transport due to forest road construction.

Acknowledgments

This research was in part funded by the Idaho Experimental Program to Stimulate Competitive Research (Award No. IIA-1301792) and the National Council for Air and Stream Improvement, Inc. (Agreement: FW-FWW-1034). We are grateful to the Potlatch Corporation for designing and implementing the MCEW site, and for providing watershed data. We thank Dr. Xi Cheng for her preliminary assessment of MCEW hydrology and Dr. Jan Boll and Jim Frankenberger for their assistance in interpreting data and providing technical guidance on WEPP modeling.

Appendix A. Supplementary material

Supplementary data to this article can be found online at https://doi.org/10.1016/j.scitotenv.2019.134877.

References

Abdelnour, A., Stieglitz, M., Pan, F., McKane, R., 2011. Catchment hydrological responses to forest harvest amount and spatial pattern. Water Resour. Res. 47, W09521. https://doi.org/10.1029/2010WR010165.

Aksoy, H., Kavvas, M.L., 2005. A review of hillslope and watershed scale erosion and sediment transport models. Catena 64, 247–271. https://doi.org/10.1016/j.catena.2005.08.008.

Al-Chokhachy, R., Black, T.A., Thomas, C., Luce, C.H., Rieman, B., Cissel, R., Carlson, A., Hendrickson, S., Archer, E.K., Kershner, J.L., 2016a. Restor. Ecol. 24, 589–598.

Al-Chokhachy, R., Black, T.A., Thomas, C., Luce, C.H., Rieman, B., Cissel, R., Carlson, A., Hendrickson, S., Archer, E.K., Kershner, J.L., 2016b. Linkages between unpaved forest roads and streambed sediment: why context matters in directing road restoration. Restor. Ecol. 24, 589–598. https://doi.org/10.1111/rec.12365.

Allen, R.G., Pereira, L.S., Reas, D., Smith, M., 1998. Crop Evapotranspiration: Guidelines for computing crop water requirement. FAO Irrig. and Drain. Pap. 56. Food and Agriculture Organization of United Nations, Rome. 300 p.

American Water Works Association, 1989. 2540 D total suspended solids dried at 103–105°C. Standard methods for the examination of water and wastewater. American Water Works Association and American Public Health Association, Washington, DC.

Anderson, C.J., Lockaby, B.G., 2011. Research gaps related to forest management and stream sediment in the United States. Environ. Manage. 47, 303–313. https://doi.org/10.1007/s00267-010-9604-1.

Arnold, J.G., Weltz, M.A., Alberts, E.E., Flanagan, D.C., 1995. Ch. 8. Plant growth component. In: Flanagan, D.C., Nearing, M.A. (Eds.), USDA-Water Erosion Prediction Project Hillslope Profile and Watershed Model Documentation. NSERL Rep. 10. USDA-ARS Nat. Soil Erosion Res. Lab, West Lafayette, Ind..

Bachmair, S., Weiler, M., 2011. New dimensions of hillslope hydrology. In: Levia, D. F., Carlyle-Moses, D., Tanaka, T. (Eds.), Forest Hydrology and Biogeochemistry. SE-23. Springer Netherlands, pp. 455–481.

Barkley, Y., Brooks, R., Keefe, R., Kimsey, M., McFarland, A., Schnepf, C., 2015. Idaho Forestry Best Management Practices Field Guide. https://www.extension.uidaho.edu/publishing/pdf/BUL/BUL891.pdf.

Bathurst, J.C., Iroume, A., 2014. Quantitative generalizations for catchment sediment yield following forest logging. Water Resour. Res. 50, 8383–8402. https://doi.org/10.1002/2014WR015711.

Beckers, J., Smerdon, B., Redding, T., Anderson, A., Pike, R., Werner, A.T., 2009. Hydrologic models for forest management applications: Part 1: Model selection. Streamline Watershed Manage. Bull. 13, 35–44.

Berenbrock, C., Tranmer, A.W., 2008. Simulation of flow, sediment transport, and sediment mobility of the lower Coeur d'Alene River, Idaho. U.S. Geol. Surv. Sci. Invest. Rep. 2008–5093, 164 p.

Bischetti, G.B., Bassanelli, C., Chiaradia, E.A., Minotta, G., Vergani, C., 2016. The effect of gap openings on soil reinforcement in two conifer stands in northern Italy. For. Ecol. Manag. 359, 286–299. https://doi.org/10.1016/j.foreco.2015.10.014.

Boggs, J., Sun, G., McNulty, S.G., 2015. Effects of timber harvest on water quantity and quality in small watersheds in the piedmont of North Carolina. J. For. 114, 27–40.

Brooks, E.S., Dobre, M., Elliot, W.J., Wu, J.Q., Boll, J., 2016. Watershed-scale evaluation of the Water Erosion Prediction Project (WEPP) model in the Lake Tahoe Basin. J. Hydrol. 533, 389–402. https://doi.org/10.1016/j.jhydrol.2015.12.004.

Bosch, J., Hewlett, J., 1982. A review of catchment experiments to determine the effect of vegetation changes on water yield and evapotranspiration. J. Hydrol. 55, 3–23.

Bourdin, D.R., Fleming, S.W., Stull, R.B., 2012. Streamflow modelling: A primer on applications, approaches and challenges. Atmosphere-Ocean 50, 507–536. https://doi.org/10.1080/07055900.2012.734276.

Bywater-Reyes, S., Bladon, K.D., Segura, C., 2018. Relative influence of landscape variables and discharge on suspended sediment yields in temperate mountain catchments. Water Resour. Res. 54, 5126–5142. https://doi.org/10.1029/2017WR021728.

Chen, C.W., Herr, J.W., Goldstein, R.A., Ice, G., Cundy, T., 2005. Retrospective comparison of watershed analysis risk management framework and hydrologic simulation program Fortran applications to mica creek watershed. J. Environ. Eng. 131, 1277–1284.

Cislaghi, A., Vergani, C., Chiaradia, E.A., Bischetti, G.B., 2019. A probabilistic 3-D slope stability analysis for forest management. In: Recent Advances in Geotechnical Research, Springer Series in Geomechanics and Geoengineering. Springer Verlag, pp. 11–21.

Conroy, W.J., Hotchkiss, R.H., Elliot, W.J., 2006. A coupled upland-erosion and instream hydrodynamic-sediment transport model for evaluating sediment transport in forested watersheds. Trans. ASABE 49, 1713–1722.

Covert, S.A., Robichaud, P.R., Elliot, W.J., Link, T.E., 2005. Evaluation of runoff prediction from WEPP-based erosion models for harvested and burned forest watersheds. Trans. ASAE 48, 1091–1100.

Doherty, J., 2005. PEST Model Independent Parameter Estimation User Manual: 5th ed. http://www.pesthomepage.org/Downloads.php#hdr1 (Accessed October 2017).

Du, E., Link, T.E., Gravelle, J.A., Hubbart, J.A., 2013. Validation and sensitivity test of the Distributed Hydrology-Soil-Vegetation Model (DHSVM) in a forested mountain watershed. Hydrol. Process. 28, 6196–6210. https://doi.org/10.1002/hyp.10110.

Du, E., Link, T.E., Liang, W., Marshall, J.D., 2016. Evaluating hydrologic effects of spatial and temporal patterns of forest canopy change using numerical modeling. Hydrol. Process. 30, 217–231. https://doi.org/10.1002/hyp.10591.

Dun, S., Wu, J.Q., Elliot, W.J., Robichaud, P.R., Flanagan, D.C., Frankenberger, J.R., Brown, R.E., Xu, A.D., 2009. Adapting the Water Erosion Prediction Project (WEPP) Model for forest applications. J. Hydrol. 336, 45–54. https://doi.org/10.1016/j.jhydrol.2008.12.019.

Eberhardt, L.L., 1976. Quantitative ecology and impact assessment. J. Environ. Manage. 4, 27–70.

Elliot, W., Miller, I.S., Hall, D., 2007. WEPP FuME analysis for a north Idaho site. In: Page-Dumroese, D., Miller, R., Mital, J., McDaniel, P., Miller, D. (Eds.), Volcanic Ash-Derived Forest Soils of the Inland Northwest: Properties and Implications for Management and Restoration. USDA For. Serv. Proc. RMRS-P-44, pp. 205–209.

Elliot, W.J., Dobre, M., Srivastava, A., Elder, K., Link, T.E., Brooks, E.S., 2016. Forest hydrology of mountainous and snow-dominated watersheds. In: Amatya, D.M., Williams, T.M., Bren, L., de Jong, C. (Eds.), Forest Hydrology: Processes, Management and Assessment. CAB International, Wallingford, UK.

Elliot, W.J., 2004. WEPP internet interfaces for forest erosion prediction. JAWRA 40, 299–309. https://doi.org/10.1111/j.1752-1688.2004.tb01030.x.

Elliot, W.J., 2013. Erosion processes and prediction with WEPP technology in forests in the Northwestern U.S. Trans. ASABE 56, 563–579. https://doi.org/10.13031/2013.42680.

Elliot, W.J., Glaza, B.D., 2008. Impacts of forest management on runoff and erosion. In: Presented at the Third Interagency Conference on Research in Watersheds, 8–11 September, 2008. Estes Park, CO, pp. 117–127. Online at https://pubs.usgs.gov/sir/2009/5049/pdf/Elliot.pdf.

Flanagan, D.C., Livingston, S.J., 1995. . USDA-Water Erosion Prediction Project User Summary USDA-ARS NSERL Rep. 11. USDA-ARS National Soil Erosion Research Laboratory, West Lafayette, IN.

Flanagan, D.C., Nearing, M.A., 1995. USDA-Water Erosion Prediction Project: Hillslope Profile and Watershed Model Documentation USDA-ARS NSERL Rep. 10. USDA-ARS National Soil Erosion Research Laboratory, West Lafayette, IN.

Flanagan, D.C., Ascough II, J.C., Nearing, M.A., Laflen, J.M., 2001. Ch. 7: The Water Erosion Prediction Project (WEPP) Model. In: Harmon, R.S., Doe, W.W. (Eds.), Landscape Erosion and Evolution Modeling. Kluwer Academic/Plenum Publishers, New York, NY, pp. 145–199.

Flanagan, D.C., Gilley, J.E., Franti, T.G., 2007. Water Erosion Prediction Project (WEPP): development history, model capabilities, and future enhancements. Trans. ASABE 50, 1603–1612.

Frankenberger, J.R., Dun, S., Flanagan, D.C., Wu, J.Q., Elliot, W.J., 2011. Development of a GIS interface for WEPP model application to Great Lakes forested watersheds ASAE Pap. 11139. ASABE, St. Joseph, Mich. http://www.fs.fed.us/rm/pubs_other/rmrs_2011_frankenberger_j001.pdf.

Garbrecht, J., Martz, L.W., 1999. TOPAZ: An automated digital landscape analysis tool for topographic evaluation, drainage identification, watershed segmentation, and subcatchment parameterization ARS Publ. No. GRL 99-1. USDA-ARS Grazinglands Research Laboratory, El Reno, OK https://www.ars.usda.gov/ARSUserFiles/60600505/agnps/dataprep/topagnps_overview.pdf.

Golden, H.E., Evenson, G.R., Tian, S., Amatya, D.M., Sun, G., 2016. Hydrological modeling in forested systems. In: Amatya, D.M., Williams, T.M., Bren, L., de Jong, C. (Eds.), Forest Hydrology: Processes, Management and Assessment. CAB International, Wallingford, UK.

Grace III, J.M., 2017. Predicting forest road surface erosion and storm runoff from high-elevation sites. Trans. ASABE 60, 705–719.

Gomi, T., Moore, R.D., Hassan, M.A., 2005. Suspended sediment dynamics in small forest streams of the Pacific Northwest. JAWRA 41, 877–897.

Gravelle, J.A., Link, T.E., 2007. Influence of timber harvesting on headwater peak stream temperatures in a Northern Idaho watershed. Forest Sci. 53, 189–205.

Gucinski, H., Brookes, M.H., Furniss, M.J., Ziemer, R.R., 2001. Forest Roads: A Synthesis of Scientific Information. PNW-GTR-509. USDA Forest Service Pacific Northwest Research Station, Portland, OR. 120 p.

Gupta, H.V., Sorooshian, S., Yapo, P.O., 1999. Status of automatic calibration for hydrologic models: comparison with multilevel expert calibration. J. Hydrol. Eng. 4, 135–143. https://doi.org/10.1061/(ASCE)1084-0699(1999) 4:2(135).

Gupta, H.V., Kling, H., Yilmaz, K.K., Martinez, G.F., 2009. Decomposition of the mean squared error and NSE performance criteria: Implications for improving hydrological modelling. J. Hydrol. 377, 80–91. https://doi.org/10.1016/j.jhydrol.2009.08.003.

Hancock, G.R., Webb, A.A., Turner, L., 2017. Sediment transport in forested head water catchments—Calibration and validation of a soil erosion and landscape evolution model. J. Hydrol. 554, 12–23.

Hassan, M.A., Church, M., Lisle, T.E., Brardinoni, F., Benda, L., Grant, G.E., 2005. Sediment transport and channel morphology of small, forested streams. JAWRA 41, 853–876.

Hatten, J.A., Segura, C., Bladon, K.D., Hale, V.C., Ice, G.G., Stednick, J.D., 2018. Effects of contemporary forest harvesting on suspended sediment in the Oregon Coast Range. Alsea Watershed Study Revisited. Forest Ecol. Manag. 408, 238–248.

He, L., Chen, J.M., Pan, Y., Birdsey, R., Kattge, J., 2012. Relationships between net primary productivity and forest stand age in U.S. forests. Global Biogeochem. Cycles 26, GB3009. https://doi.org/10.1029/2010GB003942.

Hubbart, J.A., Link, T.E., Gravelle, J.A., Elliot, W.J., 2007a. Timber harvest impacts on water yield in the continental/maritime hydroclimatic region of the United States. Forest Sci. 53, 169–180.

Hubbart, J.A., Kavanagh, K.L., Pangle, R., Link, T.E., Schotzko, A., 2007b. Cold air drainage and modeled nocturnal leaf water potential in complex forested terrain. Tree Physiol. 27, 631–639.

Istanbulluoglu, E., Tarboton, D.G., Pack, R.T., Luce, C.H., 2004. Modeling of the interactions between forest vegetation, disturbances, and sediment yields. J. Geophys. Res. 109, F01009. https://doi.org/10.1029/2003JF000041.

Jones, J.A., Post, D.A., 2004. Seasonal and successional streamflow response to forest cutting and regrowth in the northwest and eastern United States. Water Resour. Res. 40, W05203. https://doi.org/10.1029/2003WR002952.

Jones, J.A., Grant, G.E., 1996. Peak flow responses to clear-cutting and roads in small and large basins, western Cascades. Oregon. Water Resour. Res. 32, 959–974.

Karwan, D.L., Gravelle, J.A., Hubbart, J.A., 2007. Effects of timber harvest on suspended sediment loads in Mica Creek, Idaho. Forest Sci. 53, 181–188.

Luce, C.H., Black, T.A., 1999. Sediment Production from Forest Roads in Western Oregon. Water Resour. Res. 35, 2561–2570.

Luce, C., Wemple, B., 2001. Introduction to special issue on hydrologic and geomorphic effects of forest roads. Earth Surf. Proc. Landf. 26, 111–113. https://doi.org/10.1002/1096-9837(200102)26:2<111::AID-ESP165>3.0.CO;2-2.

Moore, R.D., Wondzell, S.M., 2005. Physical hydrology and the effects of forest harvesting in the Pacific Northwest: a review. JAWRA 41, 763–783.

Moriasi, N., Arnold, J.G., Van Liew, M.W., Bingner, R.L., Harmel, R.D., Veith, T., 2007. Model evaluation guidelines for systematic quantification of accuracy in watershed simulations. Trans. ASAE 50, 885–900.

Nash, J., Sutcliffe, J.V., 1970. River flow forecasting through conceptual models part I—A discussion of principles. J. Hydrol. 10, 282–290.
Ni, J.J., Leung, A.K., Ng, C.W.W., 2019. Modelling effects of root growth and decay on soil water retention and permeability. Can. Geotech. J. 56, 1049–1055. https://doi.org/10.1139/cgj-2018-0402.
Nicks, A.D., Lane, L.J., Gander, G.A., 1995. . Ch. 2. Weather generator. In: Flanagan, D. C., Nearing, M.A. (Eds.), USDA-Water Erosion Prediction Project Hillslope Profile and Watershed Model Documentation. NSERL Rep. No. 10. USDA-ARS Nat. Soil Erosion Res. Lab, West Lafayette, IN.
O'Loughlin, C.L., 1974. The effect of timber removal on the stability of forest soils. J. Hydrol. NZ 13, 121–134.
Qu, Y., Zhuang, Q., 2018. Modeling leaf area index in North America using a process-based terrestrial ecosystem model. Ecosphere 9. https://doi.org/10.1002/ecs2.2046.
Rackley, J., Chung, W., 2008. Incorporating forest road erosion into forest resource transporting planning: a case study in the Mica Creek Watershed in Northern Idaho. Trans. ASABE 51, 115–127.
Ritter, A., Muñoz-Carpena, R., 2013. Performance evaluation of hydrological models: statistical significance for reducing subjectivity in goodness-of-fit assessments. J. Hydrol. 480, 33–45. https://doi.org/10.1016/j.jhydrol.2012.12.004.
Robichaud, P.R., Brown, R.E., 2002. Silt fences: An economical technique for measuring hillslope soil erosion. Gen. Tech. Rep. RMRS-GTR-94. U.S. Department of Agriculture Forest Service, Rocky Mtn. Res. Stn. 24, Fort Collins, CO. 10.2737/RMRS-GTR-94.
Robichaud, P.R., 2000. Fire effects on infiltration rates after prescribed fire in Northern Rocky Mountain forests, USA. J. Hydrol. 231, 220–229. https://doi.org/10.1016/S0022-1694(00)00196-7.
Robichaud, P.R., Elliot, W.J., Pierson, F.B., Hall, D.E., Moffet, C.A., Ashmun, L.E., 2007. Erosion Risk Management Tool (ERMiT) User Manual Gen. Tech. Rep. RMRS-GTR-188. USDA-FS, Moscow, ID.
Runkel, R.L., Crawford, C.G., Cohn, T.A., 2004. Load Estimator (LOADEST): A FORTRAN Program for Estimating Constituent Loads in Streams and Rivers, U. S. Geol. Surv. Tech. and Meth., Bk. 4, Ch. A5, 69 p. U.S. Geol. Surv, Denver, CO.
Sánchez-Murillo, R., Brooks, E.S., Elliot, W.J., Gaze, E., Boll, J., 2014. Baseflow recession analysis in the inland Pacific Northwest of the United States. Hydrogeol. J. 23, 287–303. https://doi.org/10.1007/s10040-014-1191-4.
Schmaltz, E.M., Van Beek, L.P.H., Bogaard, T.A., Kraushaar, S., Steger, S., Glade, T., 2018. Strategies to improve the explanatory power of a dynamic slope stability model by enhancing land cover parameterization and model complexity. Earth Surf. Process. Landf. 44, 1259–1273. https://doi.org/10.1002/esp.4570.
Schnorbus, M., Alila, Y., 2013. Peak flow regime changes following forest harvesting in a snow-dominated basin: Effects of harvest area, elevation, and channel connectivity. Water Resour. Res. 49, 517–535. https://doi.org/10.1029/2012WR011901.
Shao, W., Yang, Z., Ni, J., Su, Y., Nie, W., Ma, X., 2018. Comparison of single- and dual-permeability models in simulating the unsaturated hydro-mechanical behavior in a rainfall-triggered landslide. Landslides 15, 2449–2464. https://doi.org/10.1007/s10346-018-1059-0.
Srivastava, A., Dobre, M., Wu, J.Q., Elliot, W.J., Bruner, E.S., Dun, S., Brooks, E.S., Miller, I.S., 2013. Modifying WEPP to improve streamflow simulation in a Pacific Northwest Watershed. Trans. ASABE 56, 603–611. https://doi.org/10.13031/2013.42691.
Srivastava, A., Wu, J.Q., Elliot, W.J., Brooks, E.S., Flanagan, D.C., 2017. Modeling of streamflow in a snow-dominated forest watershed using the Water Erosion Prediction Project (WEPP) model. Trans. ASABE 60, 1171–1187. https://doi.org/10.13031/trans.12035.
Srivastava, A., Wu, J.Q., Elliot, W.J., Brooks, E.S., Flanagan, D.C., 2018. A simulation study to estimate effects of wildfire and forest management on hydrology and sediment in a forested watershed, Northwestern U.S. Trans. ASABE 61, 1579–1601. https://doi.org/10.13031/trans.12326.
Stednick, J., 1996. Monitoring the effects of timber harvest on annual water yield. J. Hydrol. 176, 79–95. https://doi.org/10.1016/0022-1694(95)02780-7.
Stednick, J.D., Troendle, C.A., 2016. Hydrological effects of forest management. In: Amatya, D.M., Williams, T.M., Bren, L., de Jong, C. (Eds.), Forest Hydrology: Processes, Management and Assessment. CAB International, Wallingford, UK.
Swank, W.T., Knoepp, J.D., Vose, J.M., Laseter, S.N., Webster, J.R., 2014. Response and recovery of water yield and timing, stream sediment, abiotic parameters, and stream chemistry following logging. In: Swank, W.T., Webster, J.R. (Eds.), Long-term Response of a Forest Watershed Ecosystem. Clearcutting in the Southern Appalachian. Oxford University Press, pp. 36–56.
Tegegne, G., Park, D.K., Kim, Y., 2017. Comparison of hydrological models for the assessment of water resources in a data-scarce region, the Upper Blue Nile River Basin. J. Hydrol. 14, 49–66. https://doi.org/10.1016/j.ejrh.2017.10.002.
Thornton, P.E., Thornton, M.M., Mayer, B.W., Wilhelmi, N., Wei, Y., Devarakonda, R., Cook, R.B., 2014. DAYMET: Daily Surface Weather Data on a 1-km Grid for North America, v2. Data set. Available on-line (http://daac.ornl.gov) from Oak Ridge National Laboratory Distributed Active Archive Center, Oak Ridge, TN, USA (accessed Jan 2017).
Troendle, C.A., MacDonald, L.H., Luce, C.H., Larsen, I.J., 2010. Fuel Management and Water Yield. In: Elliot, W.J., Miller, I.S., Audin, L. (Eds.), Cumulative Watershed Effects of Fuel Management in the Western United States. Gen. Tech. Rep. RMRS-GTR-231. USDA Forest Service, Rocky Mtn. Res. Stn., Fort Collins, CO, pp. 126–148.
Troendle, C.A., Wilcox, M.S., Bevenger, G.S., Porth, L.S., 2001. The Coon Creek water yield augmentation project: Implementation of timber harvesting technology to increase streamflow. Forest Ecol. Manag. 143, 179–187.
Terwilliger, V.J., 1990. Effects of vegetation on soil slippage by pore pressure modification. Earth Surf. Process. Landf. 15, 553–570. https://doi.org/10.1002/esp.3290150607.
USDA NRCS, 2016. SNOTEL Data and Products. USDA Natural Resources Conservation Service, Washington, D.C. http://www.wcc.nrcs.usda.gov/snotel/ (accessed May 2017).
USDA NRCS, 2014. Web Soil Survey. USDA Natural Resources Conservation Service, Washington, D.C. http://websoilsurvey.nrcs.usda.gov (accessed May 2017).
Waichler, S.R., Wemple, B.C., Wigmosta, M.S., 2005. Simulation of water balance and forest treatment effects at the H.J. Andrews Experimental Forest. Hydrol. Process. 19, 3177–3199.
Wang, L., Wu, J.Q., Elliot, W.J., Feidler, F.R., Lapin, S., 2014. Linear diffusion-wave channel routing using a discrete Hyami convolution method. J. Hydrol. 509, 282–294. https://doi.org/10.1016/j.jhydrol.2013.11.046.
Wemple, B.C., Grant, G.E., 1996. Channel network extension by logging roads in two basins, western Cascades, Oregon. Water Resour. Bull. 32, 1195–1207.
Wemple, B.C., Jones, J.A., 2003. Runoff production on forest roads in a steep, mountain catchment. Water Resour. Res. 39, 1220. https://doi.org/10.1029/2002WR001744.
Williams, J.R., Dyke, P.T., Jones, C.A., 1983. EPIC-A model for assessing the effects of erosion on soil productivity. In: Proc, 3rd Int. Conf. State-of-the-Art Ecol. Model., Colorado State Univ., May 24–28, 1982, pp. 553–572.
Yang, Z., Cohen, W., Harmon, M., 2005. Modeling early forest succession following clear-cutting in western Oregon. Can. J. For. Res. 35, 1889–1900.
Ypsilantis, W.G., 2011. Upland soil erosion monitoring and assessment: An overview Tech Note 438. Bureau of Land Management, National Operations Center, Denver, CO.
Ziegler, A.D., Negishi, J.N., Sidle, R.C., Noguchi, S., Nik, A.R., 2006. Impacts of logging disturbance on hillslope saturated hydraulic conductivity in a tropical forest in Peninsular Malaysia. CATENA 67, 89–104. https://doi.org/10.1016/j.catena.2006.02.008.